Rainforest-like atmospheric chemistry in a polluted megacity

Supplementary Info.

Filtering data for mean diurnal plots – Figure 2

Diurnal plots of inorganic and organic species are shown in Figure 2 of the main manuscript for 'typical' chemistry days, i.e. where ozone increases through the morning to an afternoon peak of > 70 ppb. This accounts for 25 of the total 34 days for which ozone measurements are available. The days removed from the analysis were 22/5, 29/5, 2/6, 6/6, 8/6, 10/6, 22/6, 23/6, 24/6. Figure S1 shows the diurnal profiles of NO and O_3 for two atypical days (22/5, 2/6), compared to the mean diurnal cycle calculated from the 25 'typical' high ozone days. On these atypical days, ozone is much lower throughout the day. Ozone mixing ratios are expected to be largely driven by transport of highly chemically processed regional air masses across the densely populated areas to the south of Beijing. Beijing air quality is significantly influenced by air-masses that have passed over regions with large cities and inhabited by more than 500 million people (Parrish et al., 2016). The 'atypical', low-ozone days occur when the city is receiving cleaner air masses from the north of Beijing. The lower ozone leads to much higher concentrations of NO during the afternoon than on high ozone days. Figure S2 shows the ozone time series for the whole campaign. Figures S3 shows NO measurements for the whole campaign by hour for the afternoon hours of 12:00 to 20:00.

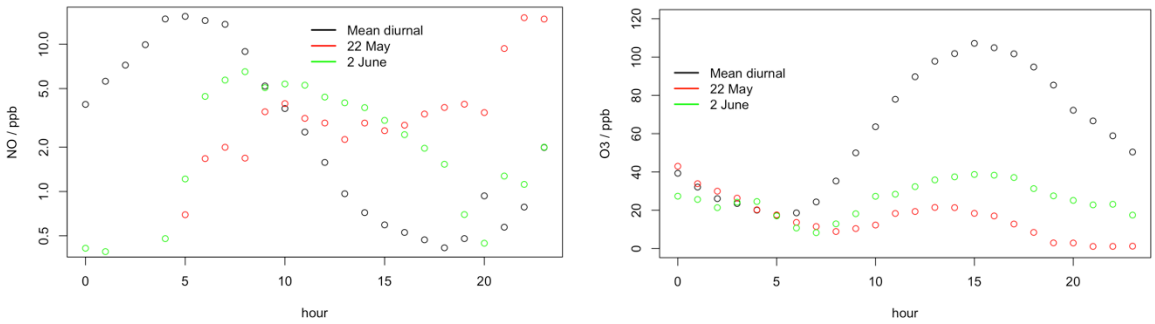

Figure S1 Comparison of mean diurnal cycle of NO and O_3 during typical high ozone days with the atypical days 22 May and 2 June. The full time series have been filtered for days with afternoon ozone peaks < 70 ppb.

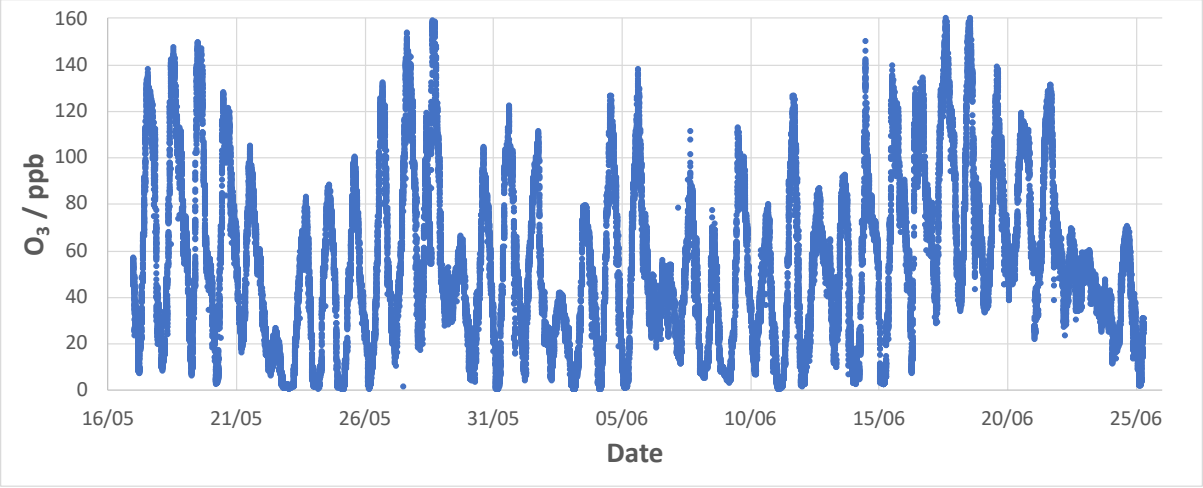

Figure S2 Ozone time series for the campaign. 17 May – 25 June.

Quantification of hourly [NO] decrease observed in the afternoon

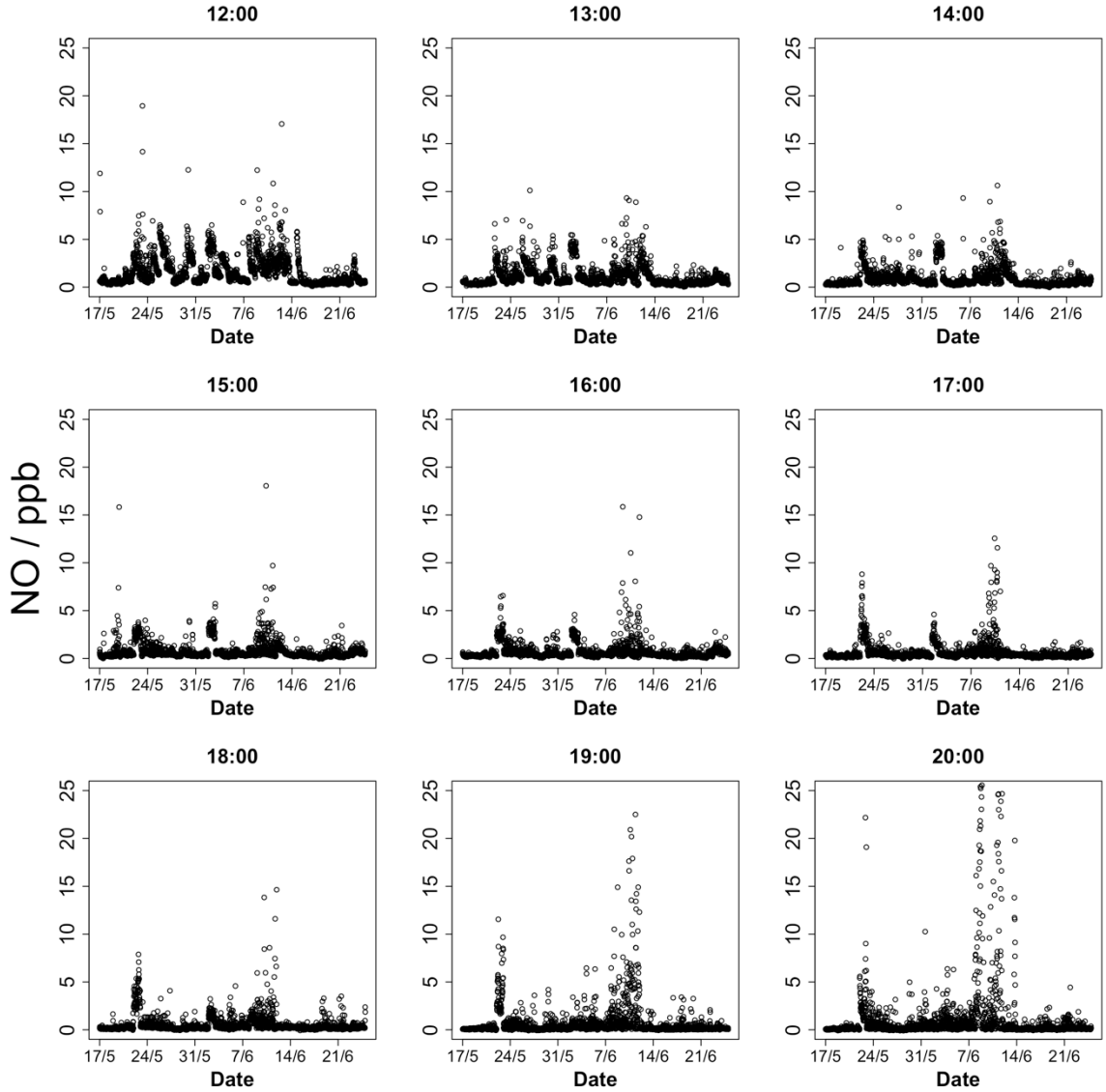

Figure S3 NO measurements for each hour between 12:00 and 20:00 for the duration of the campaign. Measurements at 1 minute frequency, i.e. 60 per day.

Figure S4 shows the mean hourly measurements of NO for each day of the campaign. A red dashed line between 12:00 and 20:00 represents the NO mixing ratio at which f_{NO} = 0.75, i.e. 25 % of ISOPOO is not reacting with NO, based on the mean hourly OH and OH reactivities for the whole campaign.

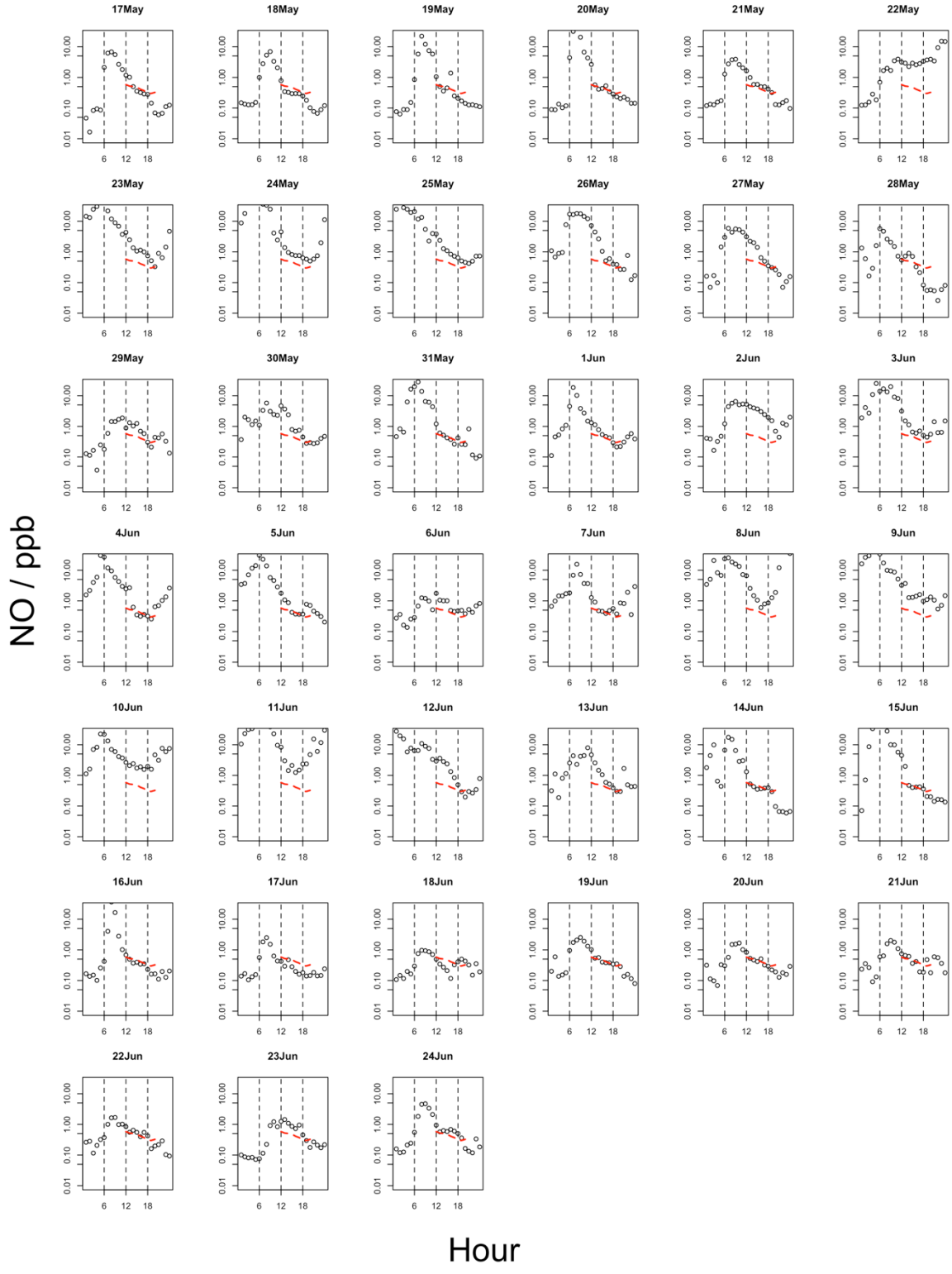

Figure S4 Mean hourly measured NO mixing ratios (ppb) during the campaign. Red dashed line between 12:00 and 20:00 represents the NO mixing ratio at which < 75 % of RO_2 are calculated to be reacting with NO.

Figure 3 Analysis

Figure 3 in the main manuscript plots measured values of [OH] $\times$ OH reactivity* against [NO] between 12:00 and 20:00 for campaigns across a range of different environments. Only field campaigns where both OH and OH reactivity were measured can be plotted on Figure 3 (see Table S1) and the variability in NO levels in these regions is likely to be greater. For the Beijing dataset, the hourly median values of [NO] are used (Figure S5), with the 9 'atypical' chemistry days (as defined above) removed. Figure S5 shows the NO measurements for each hour between 12:00 and 20:00 for the whole campaign (excluding the 9 'atypical chemistry days) binned into 50 ppt bins between 0 and 1000 ppt. The median value takes into account all of the measurements including those above 1000 ppt not shown.

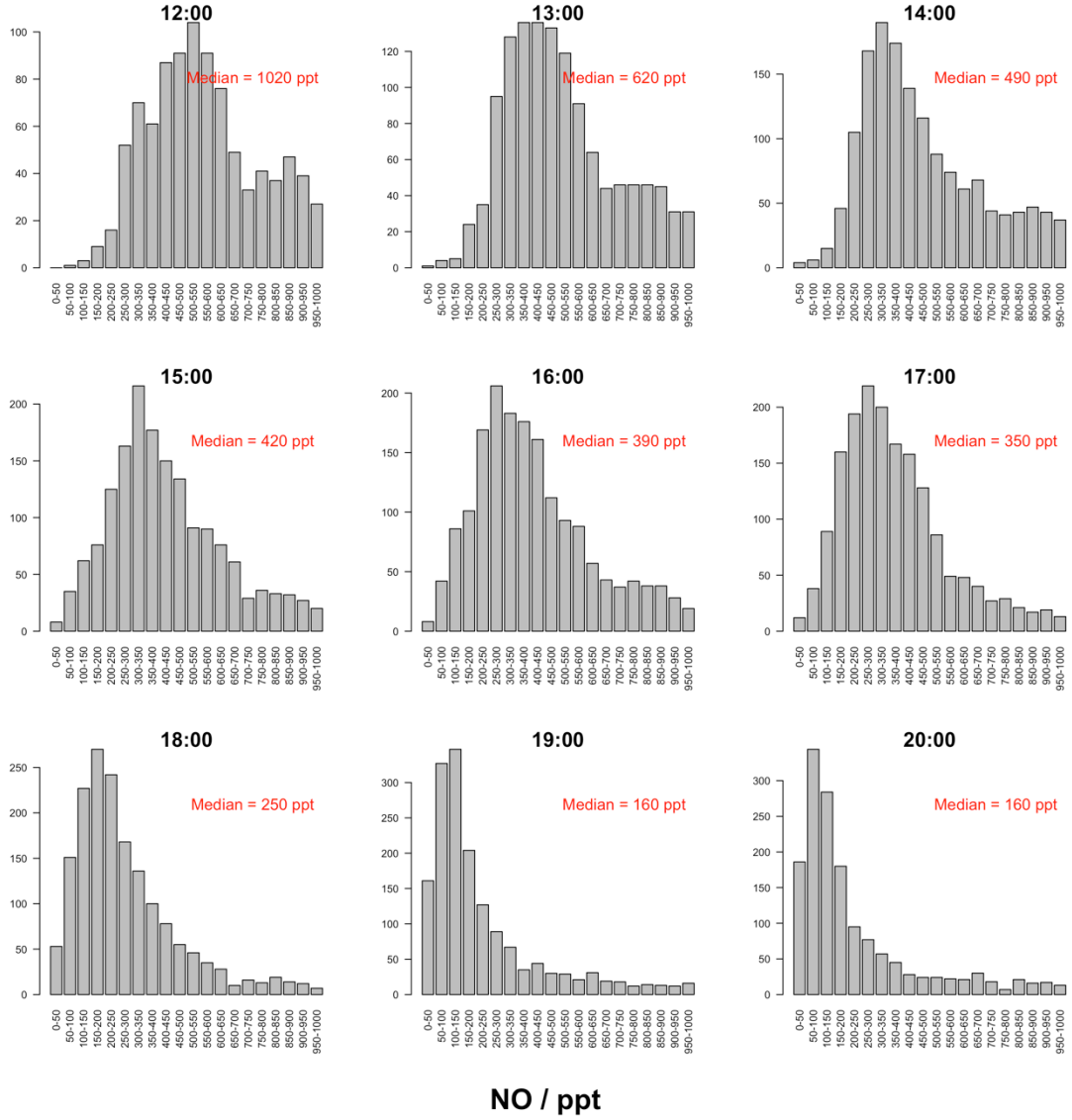

Figure S5 Distribution of minute averaged NO mixing ratios (ppt) during the campaign split in to 50 ppt bins for the hours 12:00 – 20:00, excluding the nine atypical days (see 'Filtering data for diurnals' above).

Table S1 details the location and measurement details of the NO, OH, and OH reactivity measurements presented in Figure 3 of the main manuscript.

Table S1 Details of measurement locations and conditions presented in Figure 3.

Location	Campaign	Date	HO_x and OH reactivity measurements Inlet position	Reference
NEW YORK Queens College, Borough of Queens (40° 44′ 15″ N, 73° 49′ 18″ W)	PMTACS - NY2001	June – August 2001	Co-located Scaffolding Tower at 6.4 m T = 279 – 308 K Average RH = 55 %	Ren et al. (2003)
BORNEO Burkit Atur GAW Station, Sabah Region (4° 58′ N, 117 ° 48″ E)	OP3 - I	April – May 2008	Co-located Container roof at 5 m T = 295 – 300 K	Whalley et al. (2011)
LONDON Sion Manning School, North Kensington (51° 31′ 61″ N, 0° 12′ 48″ W)	ClearfLo	July – August 2012	Co-located Container roof at 3.5 m T = 285 – 300 K	Whalley et al. (2016)
ALABAMA Centreville Research Site, Brent, SE – US (32° 54′ 11.81″ N, 87° 14″ 59.79″ W)	SOAS	June – July 2014	Co-located Tower at 15 m T = 301 – 303 K RH = 50 – 80 %	Sanchez et al. (2018)

Modelling approach

Box modelling

Table S2 Dry deposition velocities applied to all species based on their functional groups – based on Nguyen et al. (2015)

Functional group / species	Dry deposition velocity (cm s^{-1})
Hydroperoxide	2.0
H_2O_2	5.2
Organic nitrate	2.0
HNO_3	3.8
Organic acid	1.0
Oxygenated VOC	1.2
Other	0.1

Figure S6 shows the amount of ISOPOO reacting with NO ($\boldsymbol{f_{NO}}$), HO_2 ($\boldsymbol{f_{HO2}}$), RO_2 ($\boldsymbol{f_{RO2}}$), or isomerising ($\boldsymbol{f_{ISO}}$), for four different model runs with different fixed concentrations of C_5H_8 (i.e. OH reactivity) and OH. The point at which the contributions of the NO (f_{NO}) and HO_2 (f_{HO2}) channels are equal increases with increasing [OH] and with increasing OH reactivity, as shown in Figure 3 of the main manuscript. Figure S7 shows the modelled HO_2 and RO_2 concentrations for the same four model runs. As expected, both HO_2 and RO_2 increase with increasing [OH] and OH reactivity – this leads to the observed changes in $\boldsymbol{f_{NO}}$ and $\boldsymbol{f_{HO2}}$ in Figure S6. At very low [NO] (< 20 ppt), $[RO_2] > [HO_2]$, although HO_2 dominates the reaction of ISOPOO because $k(\text{ISOPOO} + HO_2) >> k(\text{ISOPOO} + RO_2)$ (Jenkin et al., 2015). As [NO] increases, $[RO_2]$ falls rapidly, with $[HO_2]$ falling less rapidly and becoming greater than RO_2.

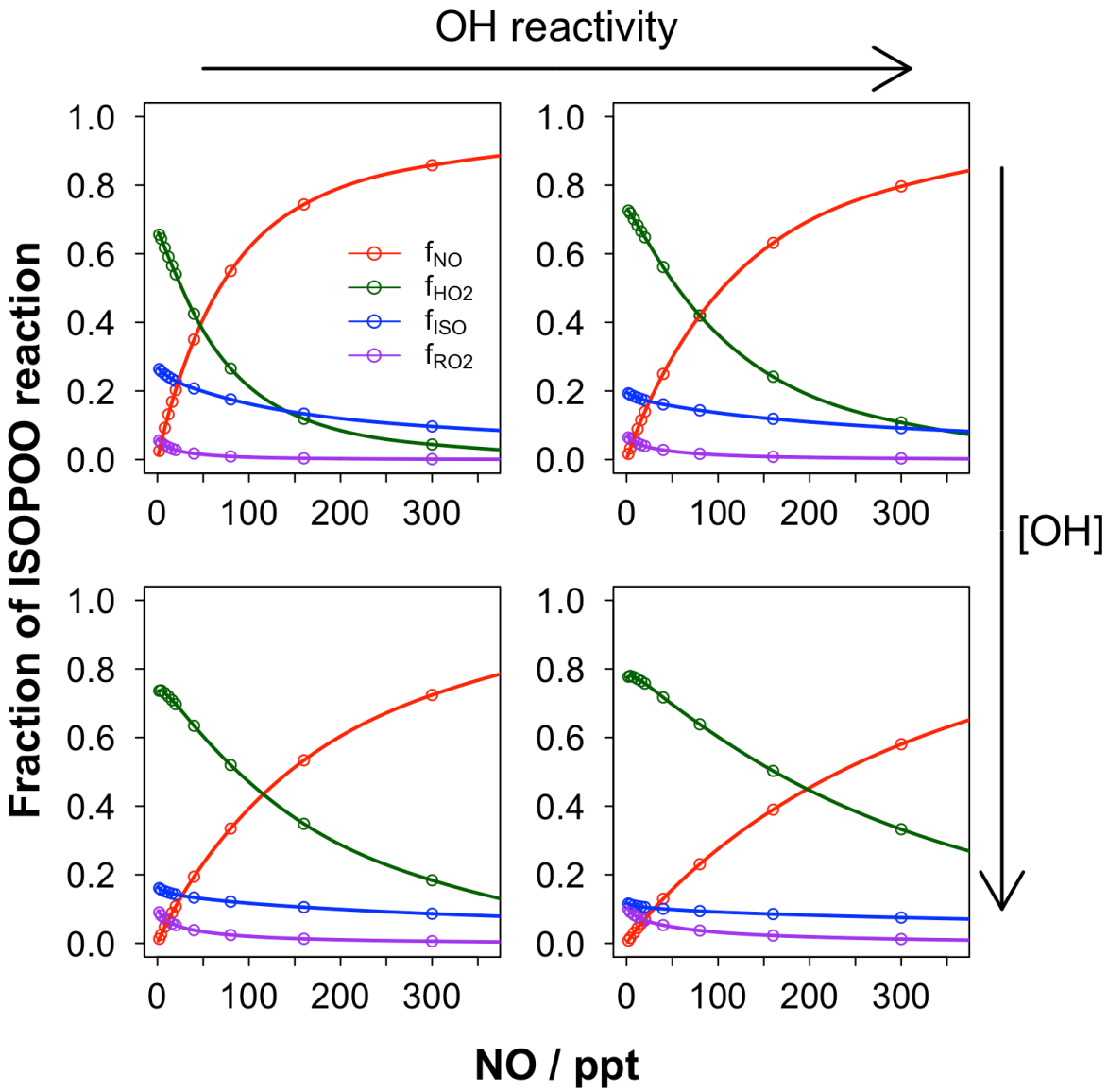

Figure S6 Example of model output showing the fraction of ISOPOO reacting with NO (f_{NO}), HO_2 (f_{HO2}), RO_2 (f_{RO2}), or isomerising (f_{ISO}), for four different model runs. Top left: $[C_5H_8]$ = 1.7 ppb, [OH] = 5×10^5 cm^{-3}; Top right: $[C_5H_8]$ = 5.0 ppb, [OH] = 5×10^5 cm^{-3}; Bottom left: $[C_5H_8]$ = 1.7 ppb, [OH] = 3×10^6 cm^{-3}; Bottom right: $[C_5H_8]$ = 5.0 ppb, [OH] = 3×10^6 cm^{-3}

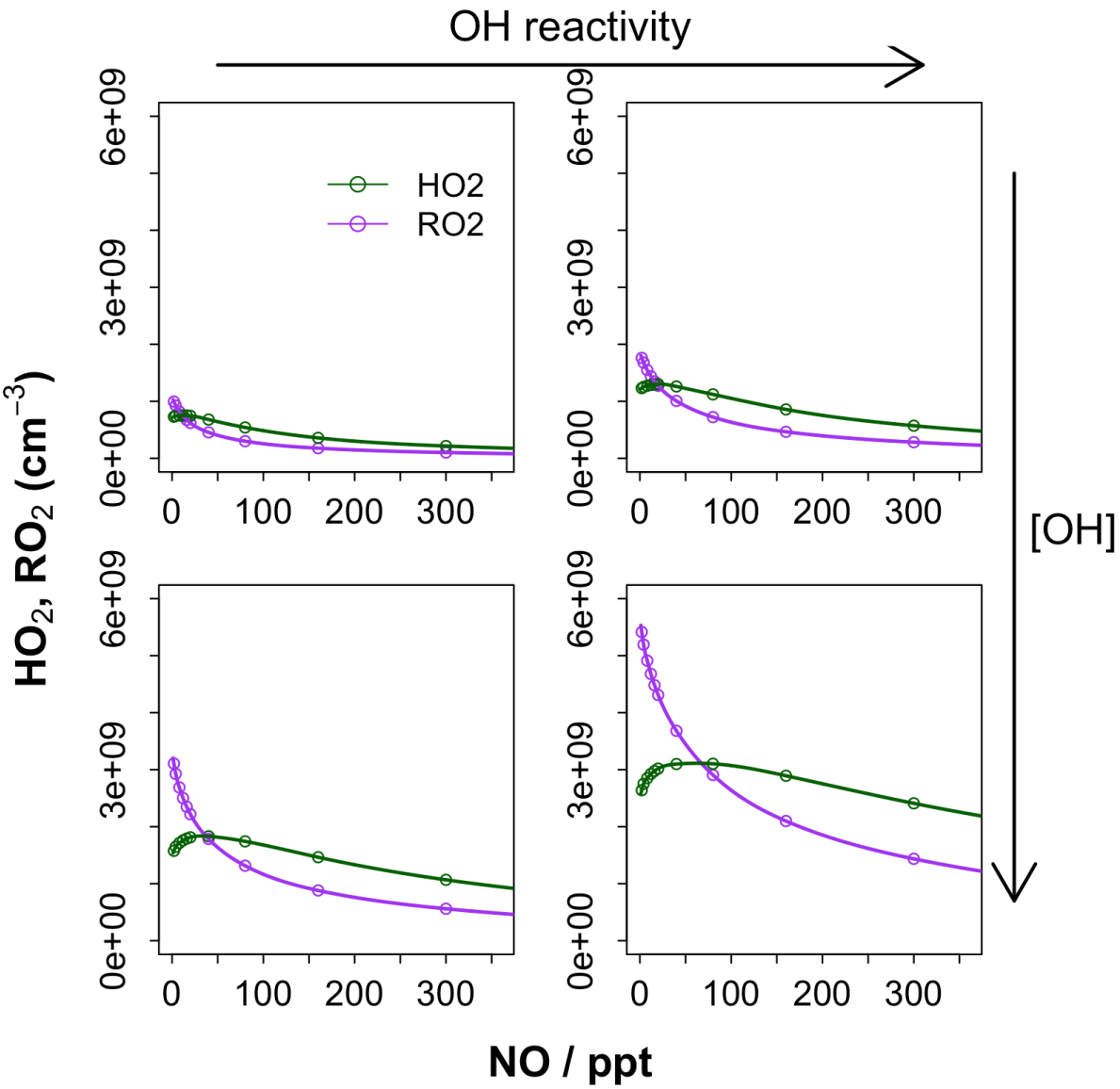

Figure S7 Example of model output showing modelled [HO_2] and [RO_2] for the four model runs shown in Figure S6. Top left: [C_5H_8] = 1.7 ppb, [OH] = 5 × 10^5 cm^{-3}; Top right: [C_5H_8] = 5.0 ppb, [OH] = 5 × 10^5 cm^{-3}; Bottom left: [C_5H_8] = 1.7 ppb, [OH] = 3 × 10^6 cm^{-3}; Bottom right: [C_5H_8] = 5.0 ppb, [OH] = 3 × 10^6 cm^{-3}

Model calculated OH reactivity

The x-axis of Figure 3 in the main manuscript is OH x OH reactivity*, where OH reactivity* is defined as the OH reactivity attributable to VOCs (Equation E1) – i.e. without contributions from OH+NO_x (as this reaction does not make any RO_2 species). The total OH reactivity as a function of [NO] from an example model run, for which [C_5H_8] = 3.4 ppb and [OH] = 1 x 10^6 cm^{-3} is shown in Figure S8. The modelled OH reactivity is highest at low NO concentrations, with the main contributions from isoprene hydroperoxides (produced from ISOPOO+HO_2) and the parent VOC isoprene. At higher NO concentrations, the reactivity first decreases as production of isoprene hydroperoxides decreases, at even higher NO concentrations, OH reactivity begins to increase again as contributions from NO and NO_2 become important – however these do not contribute to OH reactivity*.

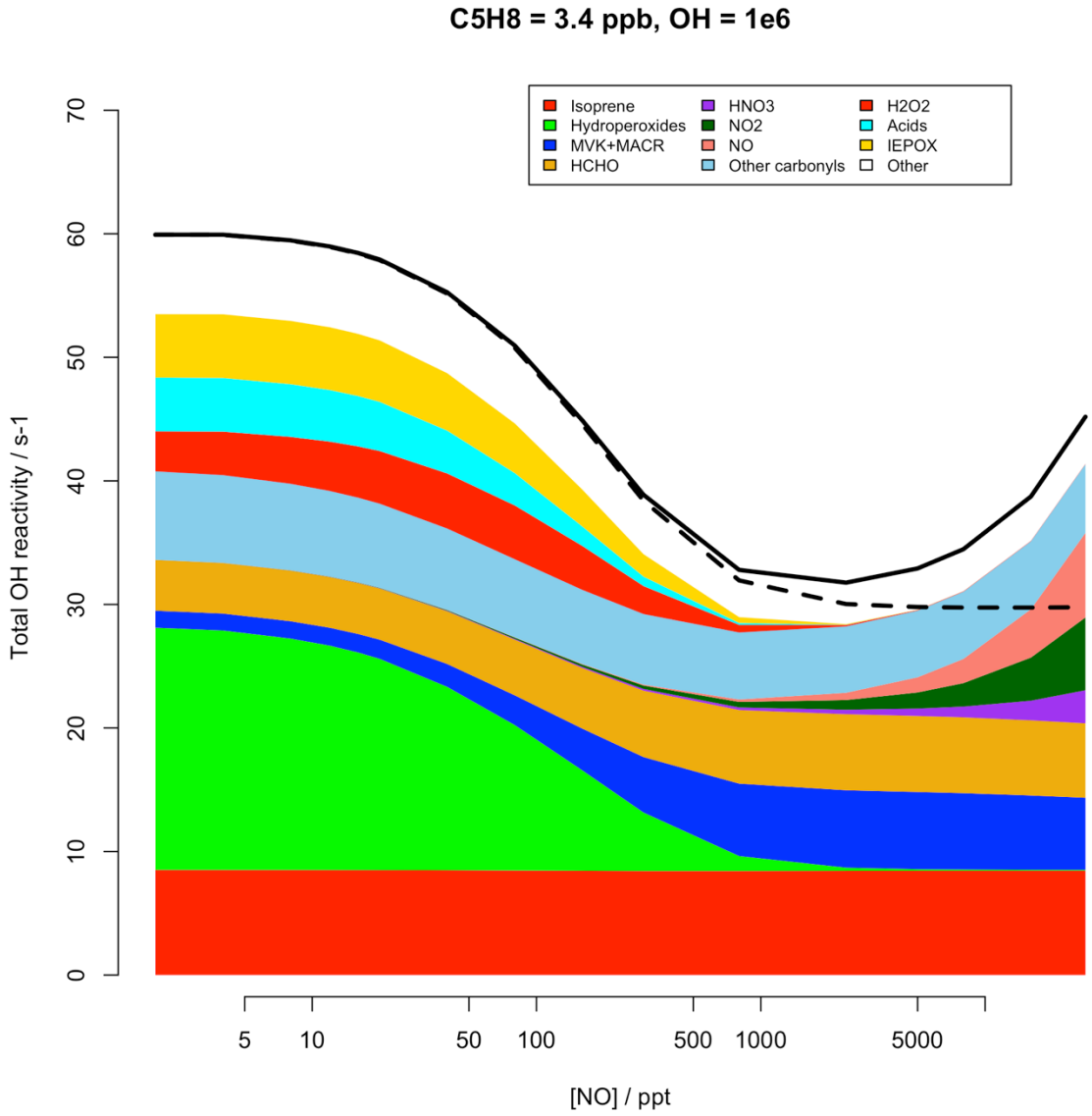

Figure S8 Modelled OH reactivity .v. [NO] for a model run initiated with [C_5H_8] = 3.4 ppbv, [OH] = 1×10^6 cm^{-3}. Solid line is total OH reactivity. Dashed line is total OH reactivity*.

Fraction of NO reacting with other RO_2

The box modelling for Figure 3 in the main manuscript is initialised with isoprene as the only VOC. Hence ISOPOO are the main (non-HO_2) RO_2 and the reactivity is dependent on isoprene and its oxidation products. However, the conclusions on the fate of ISOPOO drawn from the modelling hold for any other peroxy radicals, with minor variations. The fraction of RO_2 from a particular VOC that reacts with NO (i.e. f_{NO}) is dependent on the ratio of its reaction rate with NO (k_{NO}) to the sum of all the loss processes (Equation ES1).

$$f_{NO} = \frac{k_{NO}[NO]}{k_{NO}[NO] + k_{HO2}[HO2] + k_{RO2}[RO2] + k_{ISOM}} \quad \text{(ES1)}$$

In the MCM, k_{NO+RO2} is the same value for the majority of RO_2, $2.7 \times 10^{-12}\ exp^{(360/TEMP)} = 9.0 \times 10^{-12}$ (298K) (with the exception of acyl-RO_2 for which it is 2.0×10^{-11} (298K) (Jenkin et al., 1997; 2019)). The other possible major sink for RO_2 under atmospheric conditions is reaction with HO_2. $k_{HO2+RO2}$ varies with carbon number in the MCM tending towards a maximum value of 2.3×10^{-11} (298K) (Jenkin et al., 1997)). Figure S9 shows the variation of f_{NO} as a function of [NO] for the initial RO_2 derived from isoprene, n-butane (a straight chain alkane), and toluene (an aromatic compound). f_{NO} follows the same trend for the RO_2 from all three VOCs. For both n-butane and toluene derived RO_2, f_{NO} is a little higher than for ISOPOO. For the example of straight chain alkanes, as the size of the alkane increases, f_{NO} would be expected to approach closer to the values for isoprene, as $k_{HO2+RO2}$ becomes faster while k_{NO+RO2} remains the same.

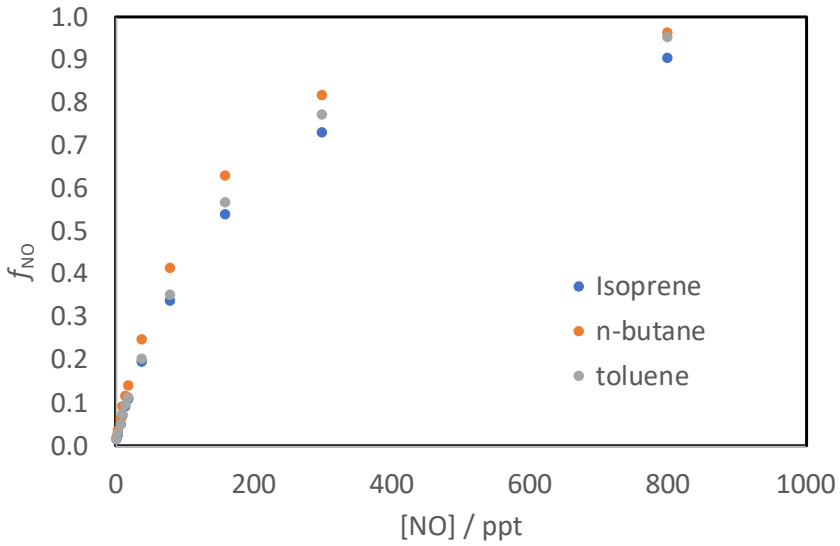

Figure S9 Variation of f_{NO} as a function of [NO] for the peroxy radicals formed in the initial OH-oxidation step of isoprene, n-butane and toluene.

GEOS-Chem Modeling

GEOS-Chem version 11-01 (http://wiki.seas.harvard.edu/geos-chem/index.php/GEOS-Chem_v11-01) with the inclusion of the aromatic component of RACM2 (regional atmospheric chemistry mechanism 2) was run nested at 0.25 x 0.3125 degree resolution, with 4 x 5 degree boundary conditions using GEOS-FP meteorology. The NO emissions were added via the default MIX emission inventory, which required a 0.9x multiplier on the total daily emissions to match observations from the APHH summer campaign. The diurnal scale factor was considerably steeper than the default GEOS-Chem NO diurnal, with a day-time scale factor on the order of 1.7x and a 0.25x night-time multiplier.

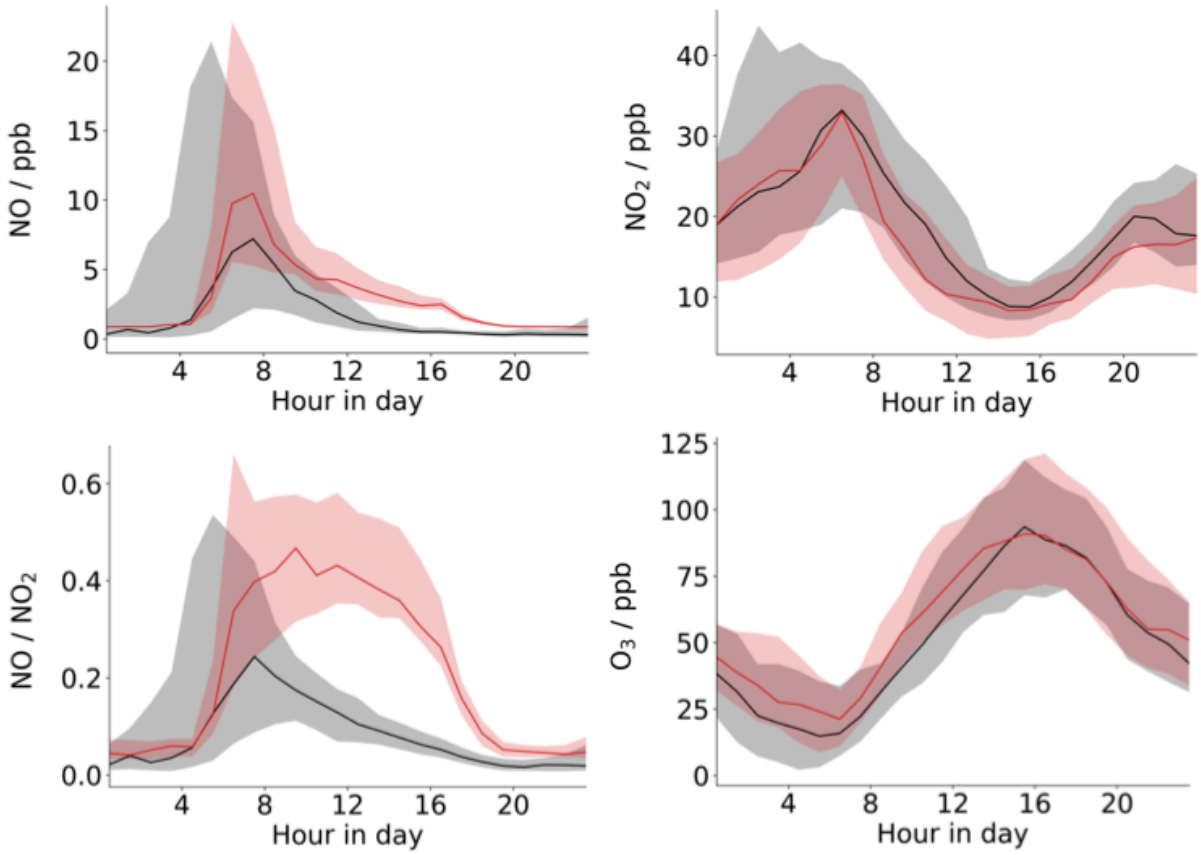

Figure S10 GEOS-Chem model output for NO, NO_2, O_3 and the NO/NO2 ratio.

While the model is able to match the observed total NO_x concentration, it cannot match the observed [NO] or NO to NO_2 ratio (Figure S10). The model over predicts NO and under predicts NO_2. The model does a good job of replicating the O_3 concentration and observed NO_2 values. As such with the chemistry currently in the model there is very little flexibility available to appreciably change this ratio.

References

Parrish D. D., Xu, J., Croes, B., and Shao, M.:Air quality improvement in Los Angeles – perspectives for developing cities, Front. Environ. Sci. Eng., 10, 2016.